Linear-Sweep Voltammetry in a Cylindrical-Pore Electrode

John W. Weidner*,† and Peter S. Fedkiw

Department of Chemical Engineering, North Carolina State University, Raleigh, North Carolina 27695-7905

A comparison is made between the transfer coefficient and standard rate constant for the oxidation of ferrous to ferric ion obtained from linear-sweep voltammetry (LSV) in a cylindrical pore drilled in a glassy-carbon disk with those obtained on a planar electrode of the same material. Extracting quantitative kinetic information from LSV in a cylindrical-pore electrode is more difficult than on planar electrodes since the electrode surface is not uniformly accessible to the bulk supply of reactant or the counter electrode. A previously reported mathematical methodology to account for the effect of ohmic, mass-transfer, and kinetic resistances on the voltammograms obtained for soluble redox couples was applied to determine the transfer coefficient and the standard rate constant for an irreversible reaction in the cylindrical pore. The transfer coefficients agreed to within 3%, but the standard rate constant was about 1 order-of-magnitude larger on the planar electrode than in the pore. This discrepancy is believed due to the difference in the pretreatment of the electrode surface rather than a failure of the model. The strongest evidence that the methodology is valid is that although the voltammogram is a strong function of the initial concentration of ferrous sulfate, the pore length, the electrolyte conductivity and the sweep rate, the kinetic constants extracted from the data were not when the suggested procedure was used.

INTRODUCTION

Linear-sweep voltammetry (LSV) has been used in conjunction with reticulated vitreous carbon electrodes,[1-3] "holey" electrodes,[4] carbon fibers,[5] and porous graphite-felt electrodes.[6] An obstacle in interpreting voltammograms from electrodes which are cylindrical pores, or a collection of pores, is that the electrode surface is not uniformly accessible to the bulk supply of reactant or the counter electrode. The mathematical methodologies that have been developed to obtain kinetic information using LSV on a planar electrode[7-10] and in a thin-layer cell[11-13] are not applicable for a cylindrical pore except in the absence of appreciable ohmic resistance and axial diffusion and at large and small sweep rates, respectively. At high sweep rates the diffusion layer is small relative to the pore diameter, and when ohmic resistance is negligible, the voltammogram has the characteristics of LSV on a planar electrode. For low sweep rates radial concentration gradients are small, and if the pore is deep, axial concentration gradients are negligible for the major fraction of the pore volume and consequently the pore behaves likes a thin-layer cell. However, at moderate sweep rates and/or in the presence of appreciable ohmic resistance and axial diffusion, LSV cannot be characterized by these two limiting cases, and the resulting voltammograms depend on the combined effects of ohmic, mass-transfer, and kinetic resistances.

In a previous communication,[14] we solved the governing material and charge conservation equations for LSV in a cylindrical-pore electrode as a model of a porous electrode. The peak currents and potentials obtained from these simulated voltammograms were correlated to measurable parameters (sweep rate, concentration of the redox species, diffusion coefficient, conductivity of the electrolyte, and pore dimensions) by making use of the planar and thin-layer theories in the high and low sweep-rate limits, respectively, and numerically solving the governing equations between the two limits. Using these correlations, a mathematical methodology was established to determine if the redox reaction kinetics are irreversible or reversible (Nernstian). If the reaction is irreversible, it was shown how the transfer coefficient α and the standard rate constant k° may be extracted from LSV data, and if the reaction is reversible how the number of electrons transferred may be deduced.

We present here an experimental confirmation of this methodology by determining the kinetic constants for the oxidation of ferrous to ferric on a glassy-carbon electrode in sulfuric acid. The kinetic constants obtained from a cylindrical-pore electrode under a variety of experimental conditions were compared to those obtained from a planar electrode of the same material.

EXPERIMENTAL SECTION

Voltammograms were measured in the three-electrode cell shown in Figure 1 under ambient conditions using an X-Y recorder (Recorder Co., Model 200). The working-electrode component is made of Kel-F (Registered trademark of 3M Corp.). Electrical contact between the glassy-carbon disk and the potentiostat was made via the stainless steel screw, and the counter electrode (CE) is platinum gauze. The removable plug and the compartment containing the reference electrode screw tight against the disk.

For the cylindrical-pore studies, a hole was drilled into two glassy-carbon disks (a 0.355 cm thick disk used in the planar study, and an additional 0.365 cm thick disk) using a carbide drill bit. Epoxy was applied to the front and back face of the disk, and after curing, the epoxy-covered surface was sanded with 600-grade silica carbide paper. The thickness of the resulting epoxy layer which confined the electroactive surface area to the inside of the pore was roughly 0.1 mm. The deep pore resulted from stacking the two disks together, but in this circumstance only the front and back face of the composite was epoxied.

The inside of the pores were polished with a 0.3-μm alumina suspension (Mark V Laboratory) using the smooth end of the carbide drill bit. The diameter of the pores changed slightly after initial polishing, but afterwards remained unchanged at 0.0715 and 0.069 ± 0.0005 cm for the deeper and shallower pores, respectively. (The diameter of the deeper pore is an average of the pore diameters from the two disks.) After rinsing twice with deionized water in an ultrasonic bath for 30 s, the pore was cleaned by pulling a Kimwipes through the pore to remove residual alumina. The disk or disks were then place in the working-electrode assembly which was subsequently filled with nitrogen-saturated 0.50 M sulfuric acid. Each sweep started at −0.20 V [all voltages are relative to the mercury sulfate electrode (MSE)] and was terminated approximately 50 mV positive of the peak current. Fe^{2+} was replenished between each sweep by removing the Kel-F plug shown in Figure 1 from the back of the working-electrode assembly which allowed drainage from the counter electrode reservoir (not shown). A total of 100 sweeps could be performed before the background current doubled, at which point the surface of the pore was repolished. The same procedure was performed to measure background currents in 0.50 M sulfuric acid.

The planar studies were performed using the glassy-carbon disk before a hole was drilled through the center and was prepared by polishing on an Alpha A cloth (Mark V Laboratory) first with

† Present address: Department of Chemical Engineering, University of South Carolina, Columbia, SC 29208.

0003-2700/92/0364-0449$03.00/0

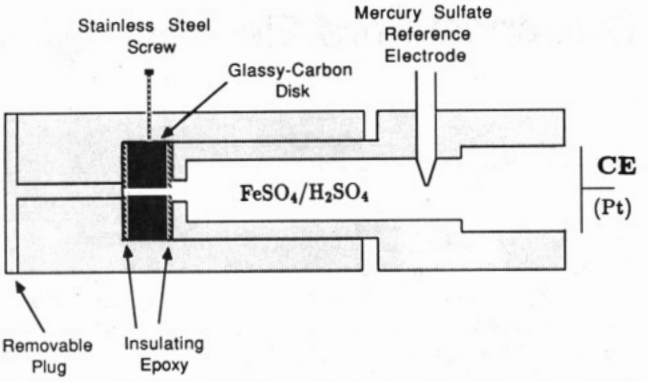

Figure 1. Schematic of the three-electrode cell used to perform LSV. The glassy-carbon disk has a cylindrical pore drilled in the center with epoxy insulating the front and back face. For planar studies, there is no pore through the disk, and no epoxy on the disk surfaces.

a 0.3-μm alumina suspension (Mark V Laboratory) and then with deionized water. The disk was rinsed twice with deionized water in an ultrasonic bath for 30 s and placed in the working-electrode assembly which was subsequently filled with deoxygenated electrolyte. The exposed area of the disk was 0.0765 cm^2. Each anodic sweep started at –0.30 V, but the potential was held at –0.60 V for approximately 15 s before the sweep was initiated in order to replenish Fe^{2+} near the electrode surface. This large cathodic potential caused the background current to double after approximately 10 sweeps, at which point the surface of the electrode was repolished. The same procedure was performed to measure background currents in 0.50 M sulfuric acid.

RESULTS AND DISCUSSION

Planar Electrode. LSV on the planar disk was performed to compare the kinetic constants obtained on this electrode with those obtained in a cylindrical pore. From planar-electrode theory[7-9] α can be determined from the peak current-vs-sweep rate data since

$$i_p = 0.4958nFAC^\circ_R\sqrt{\alpha nf\nu D} \quad (1)$$

where i_p is the peak current, n is the number of electrons transferred, F is Faraday's constant, A is the electrode area, C°_R is the initial concentration of the reduced species, $f = F/RT$, R is the gas constant, T is the temperature, ν is the sweep rate, and D is the diffusion coefficient of the reduced species. Both kinetic constants can be determined from the peak potential-vs-sweep rate data since

$$E_p^* \equiv nf(E_p - E^{\circ\prime}) = \frac{1}{\alpha}\left[0.780 + \ln\left(\frac{\sqrt{\alpha nfD}}{k^\circ}\right) + \ln\sqrt{\nu}\right] \quad (2)$$

where E_p and $E^{\circ\prime}$ are the peak and formal potentials, respectively.

Voltammograms were recorded at nine sweep rates ranging from 4 to 100 mV/s at each of six ferrous sulfate concentrations (5–100 mM). We measured a diffusion coefficient for Fe^{2+} in 0.50 M sulfuric acid of 0.50×10^{-5} cm/s using limiting-current data at a platinum rotating disk electrode and the Levich equation.[15] This agreed to within 2% with the diffusion coefficient reported by Adams[16] in 1.0 M sulfuric acid. The formal potential for the ferrous/ferric redox couple in 1.0 M sulfuric acid is 0.0 V.[17]

A plot of the peak current versus the square root of the sweep rate produced a straight line for all six concentrations and gave an average α of 0.29 ± 0.03 (the uncertainty in the results reported throughout this paper are ± one standard deviation). A plot of the peak potential versus the logarithm of the sweep rate produced a straight line for five of the six concentrations. The peak-potential data obtained at [$FeSO_4$] = 100 mM did not produce a straight line, which we attribute to appreciable uncompensated potential drop between the working and reference electrodes. The maximum current at this concentration was ~800 μA, and therefore ~800 μA is considered the maximum current at which uncompensated resistance can be ignored in this cell when 0.50 M sulfuric acid is used as the electrolyte. From the peak-potential data at the five ferrous sulfate concentrations between 5 and 50 mM, an average α of 0.30 ± 0.02 and an average k° of 80 ± 40 × 10^{-6} cm/s were obtained.

Cylindrical-Pore Electrode. There are three dimensionless parameters which govern irreversible voltammograms in a cylindrical-pore electrode:[14] $\sigma \equiv d^2nf\nu/4D$, $\gamma \equiv 2L/d$, and $\Theta \equiv 2n^{5/2}F f^{3/2}L^2C^\circ_R\sqrt{\nu D}/d\kappa$ where κ is the conductivity of the electrolyte and d and L are the pore diameter and length, respectively. The parameter σ is a dimensionless sweep rate with the voltammogram having the characteristics of LSV on a planar electrode and thin-layer cell at large and small σ, respectively. The voltammogram is only a function of the length-to-radius ratio γ at low sweep rates where axial concentration gradients are significant for a major fraction of the pore volume. Criteria were developed for which axial diffusion may be ignored,[14] and for the results reported here the voltammogram is not a function of γ. The parameter Θ is a measure of the effect to which ohmic resistance influences the voltammogram. In our previous study,[14] we found that for $\Theta \le 0.53/\alpha^{1.5}$ the peak current decreased by less than 2% and for an anodic reaction the peak potential shifted to more positive potentials by less than $1/n\alpha$ mV (T = 298 K) relative to the case where ohmic resistance is negligible (Θ = 0). For larger values of Θ, ohmic distortion is significant. For example, at $\Theta = 20/\alpha^{1.5}$ the peak current decreases by 40% and the peak potential shifts as much as $130/n\alpha$ mV (T = 298 K) from that at Θ = 0. For even larger values of Θ the voltammogram becomes so severely distorted that performing LSV beyond this point is of little practical use.

When the conditions for negligible ohmic resistance and axial diffusion are met, LSV is only a function of σ for a given set of kinetic constants. The peak currents and potentials obtained from the simulations of an anodic voltammogram were correlated to σ, α, and k°, and the resulting empirical equations are[14]

$$\left(\frac{\nu}{\hat{i}_p}\right)^{1.81} = (1.56nFdLC^\circ_R\sqrt{\alpha nfD})^{-1.81}\nu^{0.905} + (0.289n^2fFd^2LC^\circ_R\alpha)^{-1.81} \quad (3)$$

$$(\nu e^{-\alpha\hat{E}_p^*})^{2.05} = \left(\frac{0.458k^\circ}{\sqrt{\alpha nfD}}\right)^{2.05}\nu^{1.025} + \left(\frac{4k^\circ}{\alpha nfd}\right)^{2.05} \quad (4)$$

where the circumflex above i_p and E_p^* indicates the peak values which would be measured if ohmic resistance and axial diffusion are negligible. As indicated by eq 3, α can be estimated from the slope and intercept of a plot of $(\nu/\hat{i}_p)^{1.81}$ versus $\nu^{0.905}$. Using the average α value obtained from the peak-current data, eq 4 can be used to obtain k° from both the slope and the intercept of a plot of $(\nu e^{-\alpha\hat{E}_p^*})^{2.05}$ versus $\nu^{1.025}$. Alternatively, an iterative procedure may be used to obtain α and k° from the peak-potential data by guessing a value for α, plotting eq 4, and determining k° from the slope and the intercept. If k°(slope) is greater or less than k°(intercept), α is increased or decreased, respectively, until the difference between the two is minimized.

In the presence of appreciable ohmic resistance, the effect of ohmic distortion must be taken into account prior to plotting the data, as suggested by eq 3 and 4. In our previous study,[14] the effect of ohmic resistance was accounted for by simulating voltammograms in the presence of a nonuniform potential distribution and then correlating the normalized peak current ($i_p/\hat{i}_p$) and the shift in the peak potential (E_p^*

Table I. Anodic Transfer Coefficient α and the Standard Rate Constant $k°$ for the Oxidation of Ferrous to Ferric Ion in Sulfuric Acid Using LSV in a Cylindrical-Pore, Glassy-Carbon Electrode

	i_p (23 runs)	E_p (18 runs)	
	α	α	$10^6k°$, cm/s
slope	0.20 ± 0.02		
intercept	0.35 ± 0.03	0.30 ± 0.02	6 ± 3
average	0.28 ± 0.03		
overall average	0.29 ± 0.03		6 ± 3

[a] The average of the indicated number of sets of runs are listed to ± one standard deviation with each run consisting of between 7 and 15 sweeps.

$-\hat{E}_p^*$) to the parameters α, σ, and Θ. The resulting empirical equations are[14]

$$(i_p/\hat{i}_p) = \{[1.184 - 0.45 \log (\alpha^{3/2}\Theta)]^{-7.0} + 1\}^{-1/7.0} \quad (5)$$

$$\alpha(E_p^* - \hat{E}_p^*) = a(\alpha^{3/2}\Theta)^b \quad (6)$$

where a and b are empirical functions of $\alpha\sigma$ given by

$$a = 0.222\left(\frac{\alpha\sigma}{9.4 + \alpha\sigma}\right) + 0.183 \quad (7)$$

$$b = 0.27\left(\frac{\alpha\sigma}{8.7 + \alpha\sigma}\right) + 0.58 \quad (8)$$

Since the degree to which ohmic distortion affects the voltammogram is a function of α, an iterative procedure which was outlined previously[14] is required in order to plot the data as suggested by eqs 3 and 4.

A total of 23 sets of runs was performed at four different ferrous sulfate concentrations (5, 20, 30, 50 mM) in 0.50 M sulfuric acid using two pore sizes (d = 0.069 cm, L = 0.355 cm; d = 0.0715 cm, L = 0.72 cm). The sweep rates ranged from 1 to 196 mV/s. Two sets of runs were also performed at 50 mM ferrous sulfate in 0.25 M sulfuric acid using the deeper pore and sweep rates ranging from 1 to 49 mV/s.

The choice of operating conditions is based on the same requirements as for a planar electrode (i.e., minimal background current and negligible uncompensated ohmic loss) in addition to requirements unique to the pore. For example, the choice of pore size was dependent on the ease of fabrication and polishing, a length-to-radius ratio in which axial diffusion could be ignored, a σ range in the transition region between planar and thin-layer behavior, and a Θ range where correction for ohmic distortion was necessary.

A summary of the kinetic constants extracted from the LSV data obtained in a cylindrical-pore electrode using eqs 3–6 is given in Table I. Each set of runs consists of between 7 and 15 peak values at various sweep rates. From the peak-current data, an average of the α values obtained from the slope of eq 3 [α(slope)], the intercept [α(intercept)], and the average of these two values [α(ave)] are listed to ± one standard deviation for 23 sets of runs. The averages of the 18 α and $k°$ values obtained from the peak-potential data are also listed to ± one standard deviation. The overall average for α was obtained by averaging the 23 α(ave) values with the 18 α values obtained from the peak-potential data.

The kinetic data were reproducible, but α(slope) from the peak-current data was 43% lower on the average than α(intercept). Some of the difference can be attributed to the error introduced by the empirical fit used to obtained eq 3 which over and under predicts α(slope) and α(intercept), respectively. For example, numerically simulating voltammograms assuming α = 0.30 and using the conditions given in this paper for which ohmic resistance is negligible result in an α(slope) and α(intercept) of 0.28 and 0.33, respectively. An average of the two α values is considered the best estimate. Therefore, the standard deviation for α(av) given in Table I is the deviation found by averaging the 23 average α.

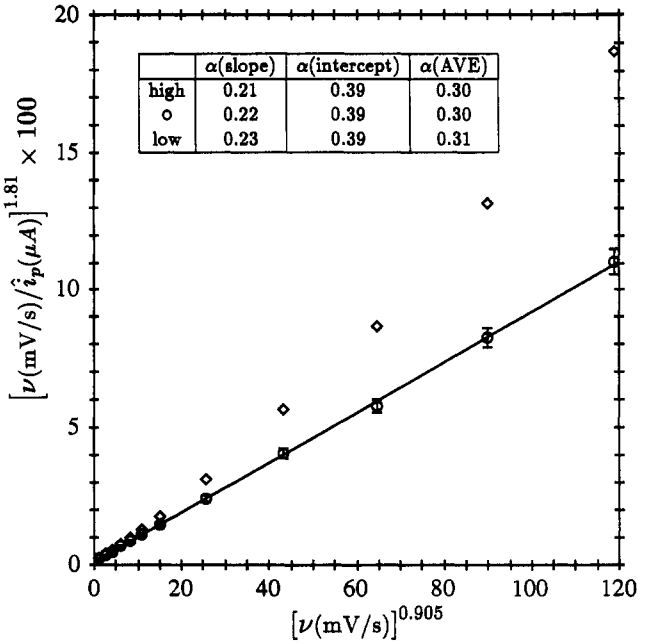

Figure 2. Peak currents plotted as suggested by eq 3. [$FeSO_4$] = 30 mM, [H_2SO_4] = 0.50 M, d = 0.0715 cm, and L = 0.72 cm. The error bars on the ohmically corrected data (O) represent a 2% uncertainty in the measured current (◇) and were obtained by correcting the maximum and minimum values for ohmic distortion. The three sets of α values result from a least-squares fit of the ohmically corrected data, and the high and low points on the error bars.

Some additional discrepancies between the two α values may result from uncertainties in the physical constants used to determine α since α(slope) is more sensitive to L, $C°_R$, and D than is α(intercept). However, these three constants are known to within 2%, which does not significantly affect the results. For example, if L or $C°_R$ was 2% lower than the value used, α(slope) would be 4% higher (0.21), and α(intercept) only 2% higher (0.36). If the diffusion coefficient was 2% lower than that used, α(slope) would be 2% lower and α(intercept) unchanged. The pore diameter is also accurate to within 2%, and α(slope) and α(intercept) are equally sensitive to this value.

Uncertainty in the physical constants which determine Θ affects the adjustments to the peak values when eqs 5 and 6 are used. For example, underestimating the effect of ohmic resistance would affect the currents at the higher sweep rates more than those at the lower sweep rates. The result would be an under prediction of α(slope) and an over prediction of α(intercept). The degree to which this would occur, however, would be a function of concentration, pore length, and electrolyte conductivity. Since α had no appreciable dependence on these variables, the discrepancy between α(slope) and α(intercept) due to the uncertainty in Θ should be minimal.

Additional uncertainty is introduced into α and $k°$ due to uncertainties in the recording of the peak currents and potentials. It was possible to record the peak currents to within 2%, regardless of the experimental conditions. Figure 2 shows the peak-current data for the case where solution resistance was the greatest (Θ = 50.5). A 2% error in the peak current corresponds to a 3.6% uncertainty in the ordinate (◇). The error bars are only shown on the ohmically-corrected data (O), so as not to clutter the graph, and were obtained by correcting the maximum and minimum raw data for ohmic distortion. The three α values listed in Figure 2 result from a least-squares fit of the ohmically-corrected data and the high and low points on the error bars. Figure 3 shows the data from Figure 2, but

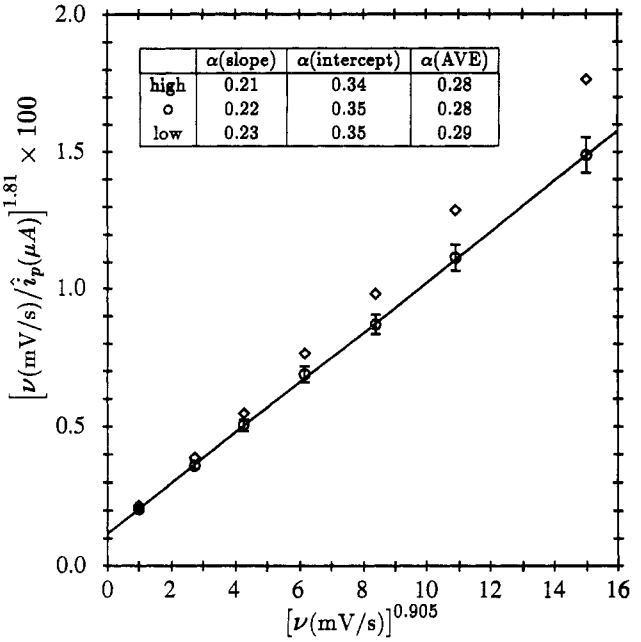

Figure 3. Peak currents plotted as suggested by eq 3. The data (◇) are the same as those in the low sweep-rate portion in Figure 2, but the error bars and the ohmically corrected data (O) were recalculated.

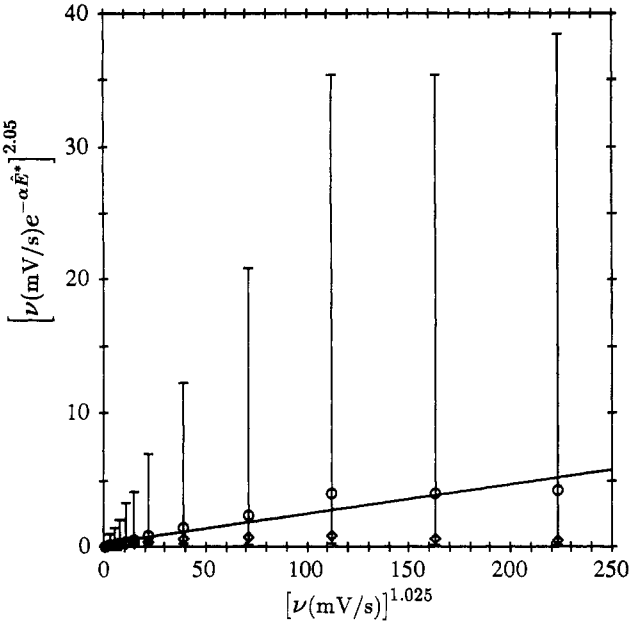

Figure 4. Peak potentials plotted as suggested by eq 4. These peak potentials correspond to the peak currents shown in Figure 2. The error bars on the ohmically corrected data (O) represent an uncertainty in the measured potentials (◇) ranging from ±2 to ±10 mV at low and high sweep rates, respectively, and were obtained by correcting the maximum and minimum values for ohmic distortion. Due to the large uncertainty in the data, no kinetic constants can be extracted.

at the low sweep rates ranging from 1 to 20 mV/s where ohmic distortion is less severe. An iterative plotting procedure was performed on these data, and the resulting α values from the slope are identical to those listed in figure 2, but the α(intercept) values are slightly smaller. It is expected that the data in Figure 3 should give a better estimate of α(intercept) since the conditions are closer to thin-layer behavior. Equation 3 reduces to LSV in a thin-layer cell as the sweep rate approaches zero.

The uncertainty in the peak potential was a strong function of ohmic distortion, as evidenced by Figures 4 and 5. For the lowest sweep rate (1 mV/s and $\Theta = 3.6$), the uncertainty in the peak potential was ±2 mV, but at the highest sweep

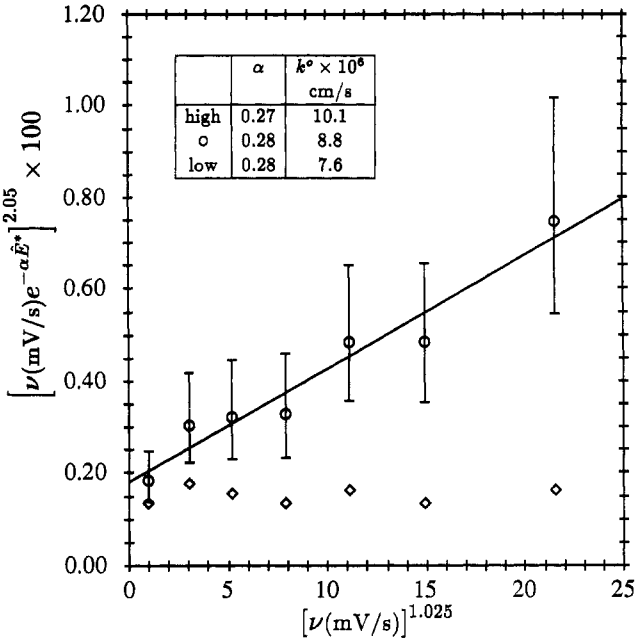

Figure 5. Peak potentials plotted as suggested by eq 4. The measured data (◇) are the same as those in the low sweep-rate portion of Figure 2, but the error bars and the ohmically corrected date (O) were recalculated. The three sets of α and k° values result from a least-squares fit of the ohmically corrected data, and the high and low points on the error bars.

rate (196 mV/s and $\Theta = 50.5$), the uncertainty was ±10 mV. The uncertainty at the high sweep rates (Figures 4) did not allow meaningful kinetic information to be extracted. Reapplying the plotting procedure for sweep rates ranging from 1 to 20 mV/s (Figures 5) allowed α and k° to be extracted as reported on the figure.

Equations 5 and 6 were developed for $\Theta \leq 20/\alpha^{1.5}$ ($\Theta \leq 120$ for $\alpha = 0.30$), and the results reported here are for $\Theta \leq 50.5$. The peak currents were useful at this value of Θ, but the peak potentials were not. The uncertainty in determining the peak potentials from the experimental voltammograms at a given Θ was greater than that from the simulated voltammograms.[14] The uncertainty in measuring the experimental peak potential sets the upper limit on Θ for which meaningful kinetic information can be extracted from peak-potential data at about 20 for $\alpha = 0.3$. Another experimental difficulty limiting the amount of ohmic distortion which is acceptable is the background current. Although the background current was insignificant for the results used to find the kinetic parameters reported here, further increasing Θ resulted in displacing the peak to more anodic potentials where the background current was significant. Background currents cannot be directly subtracted from the measured current in the presence of appreciable ohmic resistance since they also contribute to the nonuniform potential distribution.

The overall average for α agrees with α obtained from the planar data to within 3%. The value for k° obtained in the pore was reproducible but 1 order-of-magnitude lower than that obtained on the planar electrode. The discrepancy is believed to be due to the difference in the pretreatment of the electrode surface which is known to affect the kinetics at a glassy-carbon electrode.[18] Ideally, identical surface pretreatment techniques should have been used. Unfortunately, the planar study was done before it was realized that the surface-cleaning technique used was not suitable for the pore study. The strongest evidence that the methodology is valid is that although the voltammogram is a strong function of the initial concentration of ferrous sulfate, the pore length, the electrolyte conductivity, and the sweep rate, the kinetic

constants α and $k°$ extracted from the data were not.

The extracted kinetic parameters would not be independent of the physical constants if the data were plotted as suggested by planar-electrode theory. For example, using LSV data in which ohmic resistance is negligible and the sweep rates range from 2 to 100 mV/s, the peak data fall along a reasonably straight line with $\alpha = 0.27$ obtained from eq 1 and $\alpha = 0.22$ and $k° = 20 \times 10^{-6}$ cm/s obtained from eq 2. Using the sweep rates from 2 to 25 mV/s does not alter the value of α from the peak-current data, but gives $\alpha = 0.19$ and $k° = 32 \times 10^{-6}$ cm/s from the peak-potential data. Using the measured data ($\diamond$) from Figures 3 and 5, but plotted as suggested by eqs 1 and 2, respectively, results in an $\alpha = 0.20$ from the peak-current data and $\alpha = 0.14$ and $k° = 72 \times 10^{-6}$ cm/s from the peak-potential data. Likewise from the raw data in Figure 2 an α value of 0.13 is obtained. The average of these data is $\alpha = 0.20 \pm 0.06$ and $k° = (40 \pm 30) \times 10^{-6}$ cm/s. Not only is the standard deviation for these data greater than that given in Table I but also there is a clear trend in the kinetic data as ohmic resistance increases; i.e., α and $k°$ decrease and increase, respectively, as Θ increases.

CONCLUSIONS

A comparison was made between the transfer coefficient and standard rate constant for the oxidation of ferrous to ferric ion obtained from LSV in a cylindrical pore drilled in a glassy-carbon disk with those obtained on a planar electrode of the same material. A previously reported methodology[14] to extract kinetic information from LSV in a cylindrical-pore electrode was applied. The transfer coefficients agreed to within 3%, but the standard rate constant was about 1 order-of-magnitude larger on the planar electrode than in the pore. This discrepancy was believed due to the difference in the pretreatment of the electrode surface rather than a failure of the methodology. The strongest evidence that the methodology is valid is that although the voltammogram is a strong function of the initial concentration of ferrous sulfate, the conductivity of the electrolyte, the pore length, and the sweep rate, both of the kinetic constants were not when the suggested procedure was used. The methodology utilized here for extracting kinetic information from LSV in a cylindrical-pore electrode allows lower electrolyte conductivities, higher sweep rates, deeper and narrower pores, and larger reactant concentrations to be used compared to those needed for planar or thin-layer theory to be valid.

ACKNOWLEDGMENT

We thank Christian L. Traynelis for his preliminary experimental work. This work was supported by a grant from the NASA-Lewis Research Center (NAG 3-649).

REFERENCES

(1) Norvell, V. E.; Mamantov, Gleb *Anal. Chem.* **1977**, *49*, 1470-1472.
(2) Zamponi, S.; Dimarino, M.; Marassi, R.; Czerwinski, A. *J. Electroanal. Chem. Interfacial Electrochem.* **1988**, *248*, 341-348.
(3) Sorrels, Janet Weiss; Dewald, Howard D. *Anal. Chem.* **1990**, *62*, 1640-1643.
(4) Porter, Marc D.; Kiwana, Theodore *Anal. Chem.* **1984**, *56*, 529-534.
(5) Porter, S. J.; DeArmitt, C. L.; Robinson, R.; Kirby, J. P.; Bott, D. C. *High Perform. Polym.* **1989**, *1*, 85-94.
(6) Golub, D.; Oren, Y. *J. Appl. Electrochem.* **1990**, *20*, 877-879.
(7) Delahay, Paul *J. Am. Chem. Soc.* **1953**, *75*, 1190-1196.
(8) Matsuda, Hiroaki; Ayabe, Yuzo. *Z. Elektrochem.* **1955**, *59*, 494-503.
(9) Nicholson, Richard S.; Shain, Irving. *Anal. Chem.* **1964**, *36*, 706-723.
(10) Weidner, John W.; Fedkiw, Peter S. *Anal. Chem.* **1990**, *62*, 875-877.
(11) Hubbard, Alan T.; Anson, Fred C. *Anal. Chem.* **1966**, *38*, 58-61.
(12) Hubbard, Alan T. *J. Electroanal. Chem. Interfacial Electrochem.* **1969**, *22*, 165-174.
(13) Hubbard, Arthur T.; Anson, Fred C. *Electroanalytical Chemistry*; Bard, Allen J., Ed.; Marcel Dekker: New York, 1970; Vol. 4.
(14) Weidner, John W.; Fedkiw, Peter S. *J. Electrochem. Soc.* **1991**, *138*, 2514-2526.
(15) Bard, Allen J.; Faulkner, L. R. *Electrochemical Methods*; John Wiley & Sons: New York, 1980; Chapter 8.
(16) Adams, Ralph N. *Electrochemistry at Solid Electrodes*; Marcel Dekker: New York, 1969; Chapter 8.
(17) *Handbook of Chemistry and Physics*, 60th ed.; Weast, Robert C., Ed.; CRC Press: Boca Raton, FL, 1980; p D-115.
(18) Kazee, Beth; Weisshaar, Duane E.; Kuwana, Theodore. *Anal. Chem.* **1985**, *57*, 2736-2739.

RECEIVED for review August 21, 1991. Accepted November 8, 1991.

CORRESPONDENCE

Homogeneous Mechanism of Ascorbic Acid Interference in Hydrogen Peroxide Detection at Enzyme-Modified Electrodes

Sir: Since the development of the first glucose oxidase (GOx) based electrochemical sensor by Clark and Lyons[1] in 1962, there has been a proliferation in the forms of this enzyme electrode for glucose assay.[2] This widespread interest may be due to the clinical,[3,4] industrial,[5,6] and hence commercial importance of such a sensor. Thus analysis of biological systems, such as blood[7] and brain fluid,[8] is a principal area of application for these electrodes. A consequent problem associated with such analyses is the presence of endogenous electroactive species, e.g., ascorbic acid (AA)[9] and uric acid,[10] which may oxidize directly on the electrode surface, contaminating the enzyme-mediated current. Since the concentrations of these interfering substances continuously change in biological tissues and fluids,[9-11] it is essential to eliminate these effects in the development of a reliable glucose sensor.

GOx is a flavoprotein which in the presence of dioxygen is responsible for the biocatalytic oxidation of glucose. The overall enzymatic reaction may be written as follows:

$$\beta\text{-D-glucose} + \text{GOx/FAD} \rightarrow \text{D-glucono-}\delta\text{-lactone} + \text{GOx/FADH}_2 \quad \text{(I)}$$

$$\text{GOx/FADH}_2 + \text{O}_2 \rightarrow \text{GOx/FAD} + \text{H}_2\text{O}_2 \quad \text{(II)}$$

Classical devices involved monitoring either the consumption of oxygen[12] or the formation of H_2O_2.[13] In the latter, most common system, the peroxide generated is detected amperometrically at an inert electrode, such as Pt or graphite. This type of sensor has several drawbacks. First, the response of the device is affected by the ambient concentration of oxygen. Second, the oxidation of peroxide is irreversible, requiring a large overpotential at which other species present in the sample can contribute to the faradaic current.

In an effort to avoid these problems, mediators (e.g., benzoquinones, naphthoquinones, ferrocenium ions, and phe-

0003-2700/92/0364-0453$03.00/0